

Chapter 2

The detectors

2.1 Detector overview

Both LHCf detectors employ two imaging shower calorimeters. While the structure of the calorimeters is similar (except for their sizes and orientation), the position sensitive sensors are quite different. Detector 1 uses scintillating fibers (SciFi) and Multi-anode PMTs (MAPMTs), while detector 2 uses silicon strip sensors. Four X-Y pairs of the position sensors are installed at 6, 10, 30 and 42 X_0 for detector 1 and 6, 12, 30 and 42 X_0 for detector 2. The first two pairs are optimized to detect the shower maximum of gamma-ray induced showers and the other two are for hadronic showers developed deep in the calorimeters. These position sensitive sensors are necessary not only to obtain the transverse momentum of the incident primary but also to correct for the effect of leakage from the edges of the calorimeters. Because the fraction of shower leakage with respect to the total energy is only a function of the position and independent of the energy, we can correct for this effect by measuring the position of the shower. Details of the shower leakage correction are found elsewhere [10].

Calorimeter components (scintillator, tungsten and PMT), position sensors and their front-end electronics are packed in a $92\text{ mm}^w \times 620\text{ mm}^h \times 280\text{ mm}^l$ aluminum box for each detector as shown in figure 2.1, 2.2, 2.3. The size is designed to fit the narrow instrumentation slot in the TAN. One wall of the box for detector 2 is made of copper to better dissipate the heat generated by the front-end circuitry for the silicon strips. The detectors in their boxes are attached to and supported by the manipulators. In front of each detector (facing the IP), a counter composed of thin plastic scintillators called the Front Counter (FC) is installed.

2.2 Calorimeter

The longitudinal (along the beam direction) structure of the calorimeter is shown in figure 2.4. Each calorimeter consists of 16 layers of tungsten plates interleaved with 3 mm thick plastic scintillators (Eljen Technology EJ-260) for measuring the deposited energy. The thickness of the tungsten plates is 7 mm for the first 11 layers and 14 mm for the rest. Including the position sensors the total length is 220 mm. In units of radiation and hadron interaction lengths the total length of a calorimeter is 44 X_0 and 1.7λ , respectively. Most of the tungsten layers are attached to holders made of G10



Figure 2.1: Photo of detector 1 (left) and detector 2 (right).

while the holders near the silicon layers are made of Delrin. All the layers are stacked together and pinned in position with two G10 rods. The transverse sizes of the calorimeters are $20\text{ mm} \times 20\text{ mm}$ and $40\text{ mm} \times 40\text{ mm}$ for detector 1 and $25\text{ mm} \times 25\text{ mm}$ and $32\text{ mm} \times 32\text{ mm}$ for detector 2. The cross sections of two detectors are shown in figure 1.4. Because of the small Moliere radius of tungsten (9 mm), electro-magnetic showers are well contained even for such small calorimeters. In addition the incident position provided by the position sensitive layers is used to correct for shower-leakage.

Each plastic scintillator is viewed by an acrylic light guide and then read out by a PMT (HAMAMATSU R7400U) through 1 mm diameter optical fibers. The signals from the PMTs are amplified by pre-amplifiers installed on the top of the TAN (amplification factor = 4.8) and sent to the counting room (USA15) through 200 m coaxial cables. Because of the light guide geometry, scintillation light is not collected uniformly over the area of a scintillator. The position dependence of light yield has been measured for each scintillator light-guide combination before detector assembly. The light yield from the scintillators was measured on a $4\text{ mm} \times 4\text{ mm}$ grid with a ^{90}Sr β -ray source through a 2 mm diameter collimator. An example of the measured non-uniformity of light yield is shown in figure 2.5. The correction of this non-uniformity was also checked with muons in a test beam at the SPS. Typical non-uniformity is about $\pm 10\%$, and is corrected in further analysis as described in section 4.2.1.

The coaxial cable of $50\ \Omega$ impedance (C-50-3-1) has a delay of 4.23 ns/m and attenuates the pulse height from the amplifiers by a factor of 5 but transfers 90% of the total charge. To obtain linearity over a wide dynamic range, the combination of scintillator and PMT have been carefully chosen. The scintillator has a long decay time (9.4 nsec) to reduce the peak current in the PMT. Also the bias resistor network of the PMT was optimized to assure a good linear response over a wide dynamic range.

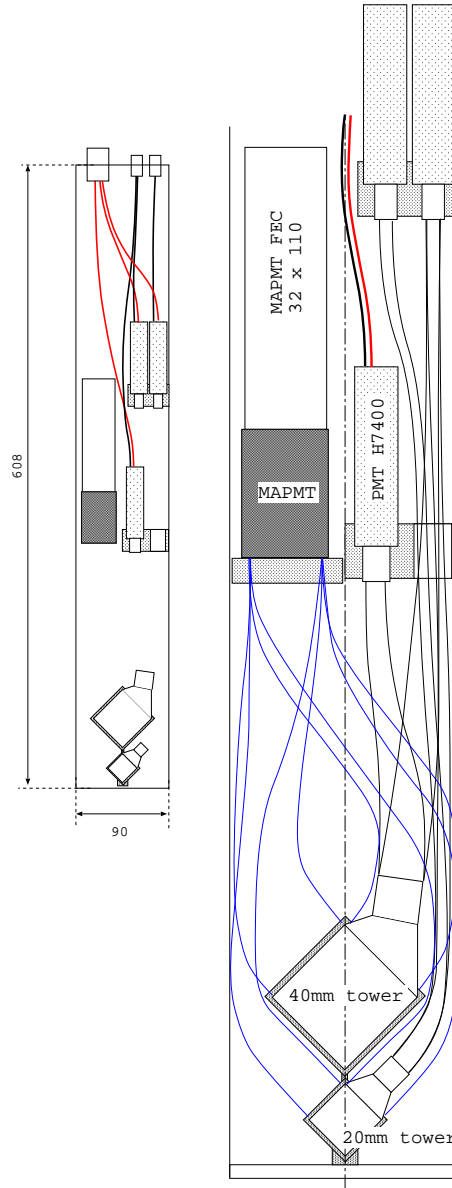


Figure 2.2: Front cut-away view of detector 1 showing the structure of the calorimeters, flexible light guide fibers, PMTs, MAPMTs front-end circuit box and inner cabling. The right figure is an enlarged view of the left one.

The linearity of the system is measured using a fast nitrogen laser (USHO KEN-1020; emission wavelength at 337 nm). Because the nitrogen laser directly excites the wavelength shifter in the scintillator with a 0.3 nsec pulse, the time profile of the scintillation light is nearly the same as that excited by a charged particle. Figure 2.6 shows the typical linearity of the PMT response with different bias HV. The modified PMT shows good linearity with a typical HV of 400 V while a single minimum ionizing particle (MIP) can be detected with about 1000 V HV.

These linearity curves have been measured for all PMT's for various values of bias HV. At typical operating HV, the linearity was checked for all the PMT's by changing the intensity of the

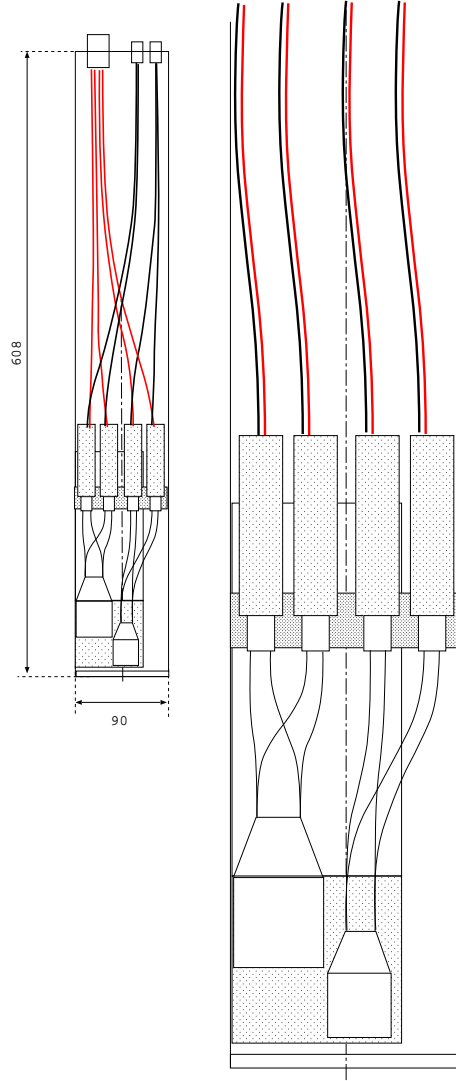


Figure 2.3: Front cut-away view of detector 2 showing the structure of the calorimeters, flexible light guide fibers, PMTs, silicon layers, their front-end circuit boards and inner cabling. The right figure is an enlarged view of the left one.

fast nitrogen laser precisely with a variety of neutral density (ND) filters. Figure 2.7 shows an example of the linearity of the PMT response. Here the horizontal axis indicates the nitrogen laser intensity in units of the equivalent number of shower particles (MIPs) detected at a layer. The vertical axis is the output of the PMT. Thus all the PMTs were checked to assure good linearity ($<5\%$ deviation) for incident light intensity varying from that corresponding to 1 MIP up to the 10^5 MIPs expected at the shower maximum of a 10 TeV γ -ray.

In order to monitor and correct for time variation of gain or radiation damage to the scintillators, a fast nitrogen laser will be installed in USA15 for periodically illuminating each scintillator through 200 m bundles of quartz fibers. Pulse to pulse variation of laser intensity is about 20% and will be monitored during the run by two dedicated PMTs at USA15.

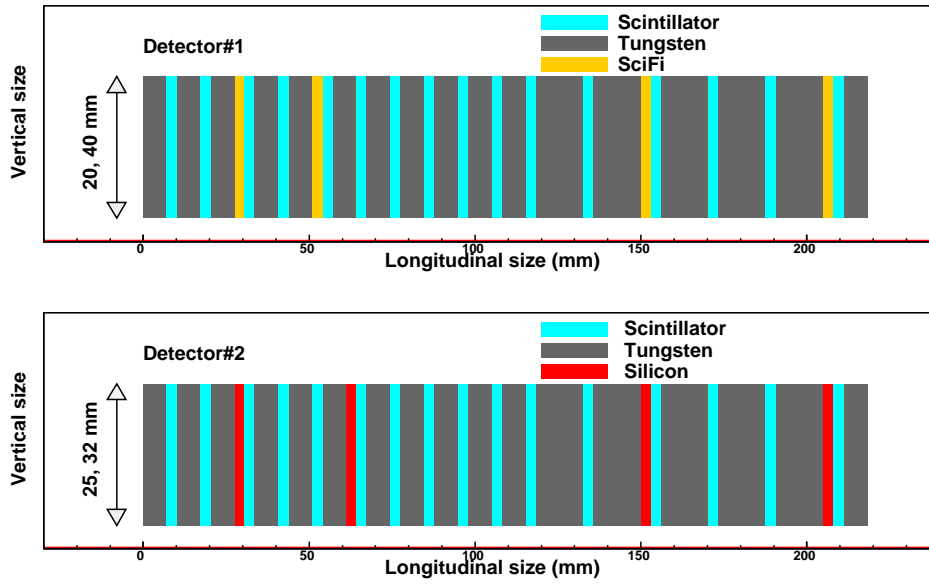


Figure 2.4: Longitudinal structure of detector 1 (top) and detector 2 (bottom); grey, light blue, orange and red indicate the layers of tungsten, plastic scintillator, SciFi and silicon strip sensor, respectively.

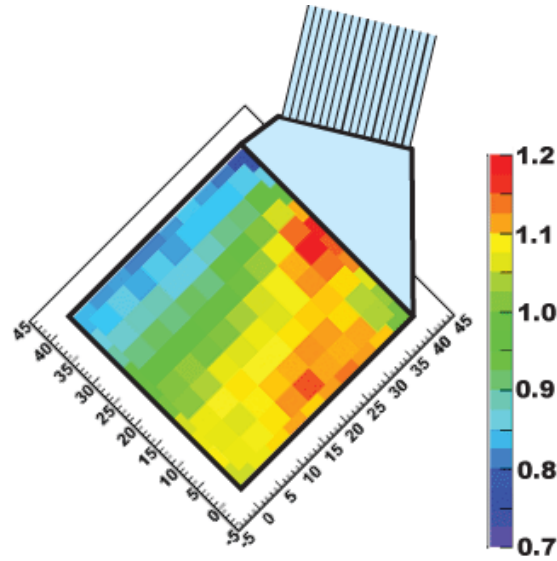


Figure 2.5: Position dependence of the light yield in a plastic scintillator. Color scale indicates relative signal intensity generated by β -rays.

2.3 SciFi and MAPMT

The position sensor of detector 1 is composed of 4 X-Y pairs of SciFi belts (KURARAY SCSF-38). A SciFi belt consists of 20 (40) SciFi's in a single hodoscope plane for the 20 mm (40 mm)

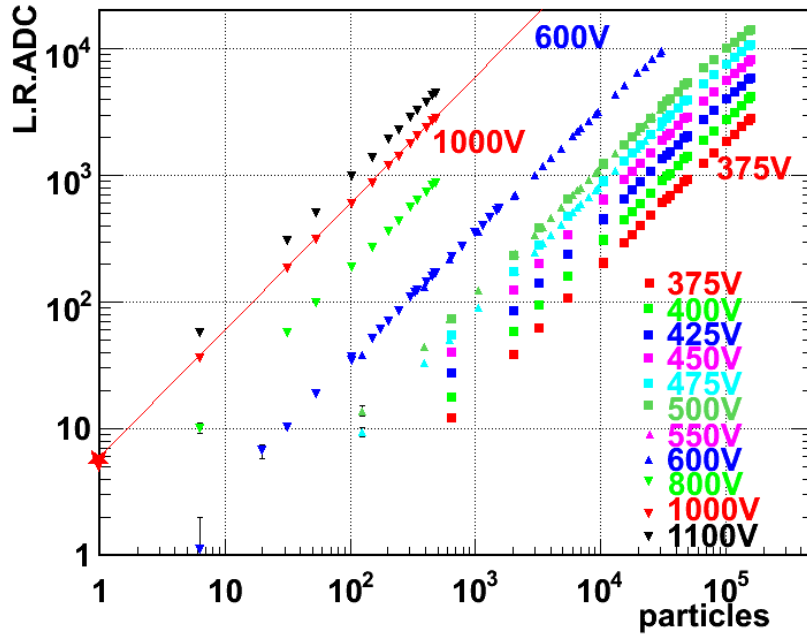


Figure 2.6: Linearity of scintillator and PMT excited by a nitrogen laser. Horizontal axis is the incident laser intensity in units of equivalent MIPs and vertical axis is AD count of the PMT output (1 AD count corresponds to 0.025 pC). Results are given for PMT HV bias from 375V to 1100V.

calorimeter. Each SciFi has 1 mm square cross-section. The SciFi belts are painted with white acrylic water paint to improve light collection efficiency, to reduce cross talk between SciFi's, and to fix the SciFi's in a plane. Because fixing the SciFi's with paint is not very strong, both surfaces of a SciFi belt are covered with kapton tape. Hodoscope planes of the 20 mm and 40mm calorimeters that are inserted in the same layer are glued on the acrylic frame (figure 2.8) and pinned together with the scintillator and tungsten layers with G10 rods. The total number of SciFi channels is 480. Each SciFi is connected channel by channel with optical cement to a clear round fiber of 1 mm diameter. The clear fiber is attached as a light guide to one of 64 anodes of a MAPMT (HAMAMATSU H7546). The SciFi photon yield of a single MIP corresponds to more than 5 photo electrons. We need 8 MAPMTs to read out 480 channels of SciFi's, so the total number of channels of the 8 MAPMTs (512) exceeds that of the SciFi's.

2.4 Silicon strip detector

The position sensor of detector2 is composed of 4 planes of microstrip silicon sensors. Each plane consists of 2 single-sided sensors, identical to those used by the ATLAS experiment for the barrel part of the Semi-Conductor Tracker (SCT) [13], which are used for the measurement of two orthogonal coordinates. These silicon sensors have $64 \text{ mm} \times 64 \text{ mm}$ total surface area, which is enough to cover the entire cross section of the calorimeter, and are produced on a $285 \mu\text{m}$ thick n-type wafer. A sequence of 768 p+ microstrips with $80 \mu\text{m}$ pitch is implanted on the junction side. The PACE3 chip, a 32 ch device designed to work with the LHC 40 MHz clock and produced for the

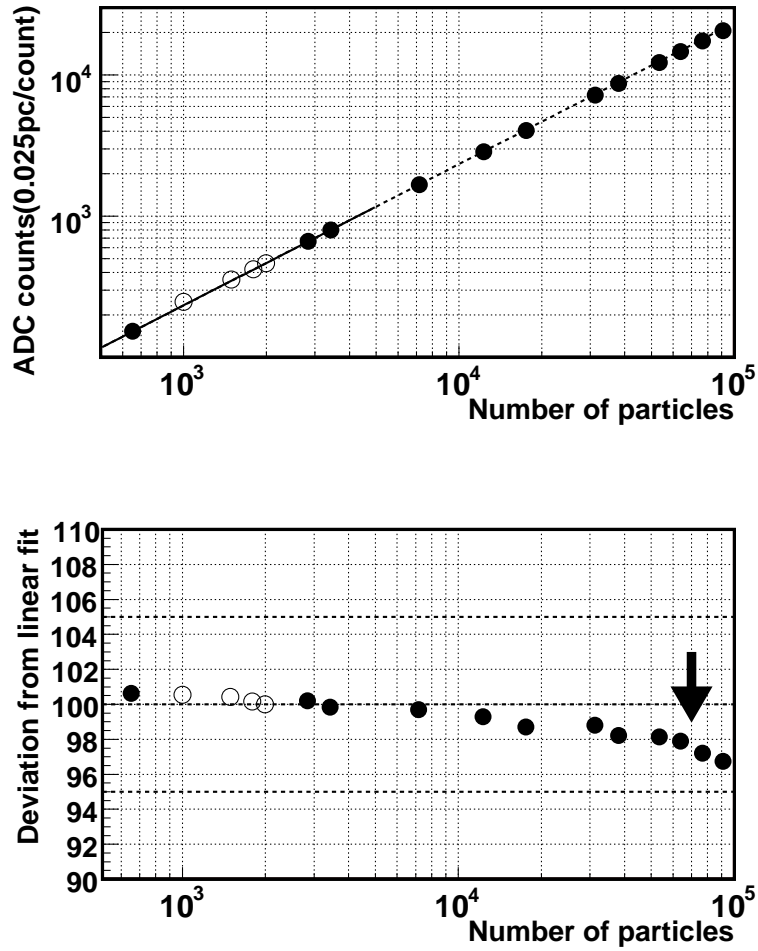


Figure 2.7: Linearity and dynamic range for one of the PMTs at nominal HV. The filled circles show the result of the laser calibration while the open circles show the result of the beam test at SPS. Horizontal axis shows relative intensity of the laser light in units of the equivalent number of MIPs determined from the beam test. The mean number of shower particles at the 7 TeV γ -ray shower maximum is indicated by an arrow.

CMS Silicon Preshower Detector [14], has been chosen for the front-end read-out. With a properly adjusted working point, the chips have a high dynamic range (up to 600 MIPs with a maximum deviation from linearity of 6%). Due to the limited space inside the TAN and the small Moliere radius in tungsten, we decided to read out every other strip; the read-out pitch is hence $160\ \mu\text{m}$. In this way we have a total of 384 channels for each silicon sensor (12 PACE3 chips, housed on two printed circuit boards). The silicon sensor is glued on a thin fiberglass fan-out circuit that is also used to provide bias to the sensor through its backplane by means of a conducting glue [15]. Microstrips on the silicon sensors have been wire-bonded to the fan-out lines in the clean room of INFN-Florence. The front-end electronics are glued to dedicated kapton fan-out circuits, that in turn are wire-bonded to the boards and to the fiberglass circuit, as shown in figure 2.9. Each tracking layer is then glued on a 0.5 mm thick aluminum layer (used for mechanical support) and

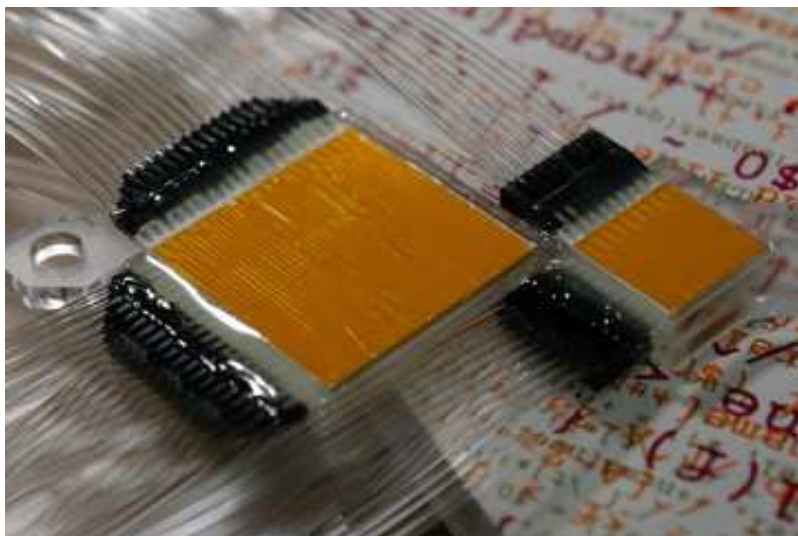


Figure 2.8: Photo of the SciFi hodoscope glued on the acrylic frame. Left and right parts are single hodoscope planes of 40 mm and 20 mm calorimeters, respectively.



Figure 2.9: Photograph of a silicon layer during the assembly phase.

covered by a black Delrin frame on the silicon and by a 8.5 mm thick aluminum frame on the circuitry part. This metal frame is also used to extract the heat produced by the chips (silicon front-end circuits dissipate approximately 60 W in total) by means of a good thermal contact with the thick copper wall used in the detector package of detector 2.

2.5 Manipulator

The manipulators move the detectors in the vertical direction in order to increase the range of P_T coverage as well as to retract the detectors from the beam line to avoid unnecessary radiation damage when data is not being taken. The manipulators can be operated remotely. Considering the limited access to the TAN area and its high radiation environment, the manipulators were designed to be as robust as possible to avoid any mechanical trouble during LHC operation. A DC motor is driven by DC power supplied from the control room. The movement direction is determined by the polarity of the power supply that is also switched in the control room. Two mechanical switches are installed at the top and bottom to limit the stroke.

The absolute position of the detector is measured by two methods. One is to use a linear optical encoder (Mutoh DS-25) with a precision of $25\ \mu\text{m}$. When the motor is driven with 15 V DC nominal voltage, the detector moves with a speed of 10 mm/min. During movement the encoder sends out two sequences of pulses with different phases. A counter installed in the counting room receives these pulses and gives the position of the detector. However, generally, optical encoders are known to be susceptible to radiation damage. Consequently a potentiometer has been prepared for a backup. The potentiometer (Mutoh RECTI P12) is simply a variable resistance with the sliding point moving with the detector. By measuring two variable resistances (R_1 and R_2) and calculating $P_{\text{pot}} = \frac{R_1}{R_1 + R_2}$, one can obtain a good position resolution. The use of a resistance ratio compensates for the possible effect of temperature change. To determine the resolution we compared the optical encoder value and P_{pot} measured at the same time for various positions. The rms deviation of the residual from a linear fit was $70\ \mu\text{m}$. This same result was obtained several times at intervals of one week.

2.6 Front counters

The FCs have a thickness of 8 mm and are inserted in front of detector 1 and detector 2. Two pairs of thin plastic scintillators ($40\text{ mm} \times 80\text{ mm} \times 2.0\text{ mm}$; Saint-Gobain Crystals BC404) are aligned in the vertical and horizontal directions to compose a double layer counter as shown in figure 2.10. Between the two layers, a copper plate of 0.5 mm thickness is inserted. Scintillation light outputs are sent through an acrylic light guide and optical fibers to four PMTs (HAMAMATSU H3164-10) placed outside of the TAN instrumentation slot. The PMT signals are sent to the counting room and recorded by ADCs. The signals are also sent to discriminators and may be used for an additional trigger information. The FC can be used to tag IP interactions with particles produced in both Arms with as wide an acceptance as possible for reducing background events produced by beam-gas interactions and beam-halo interactions with the beam pipe upstream of the TAN. The FC can also be used in anti-coincidence mode to ensure that neutral particles are being detected by the calorimeters and not charged particle background produced by beam-gas and beam-halo interactions. Using the segmented structure of the FC, we also expect a certain level of position measurement of incident particles.

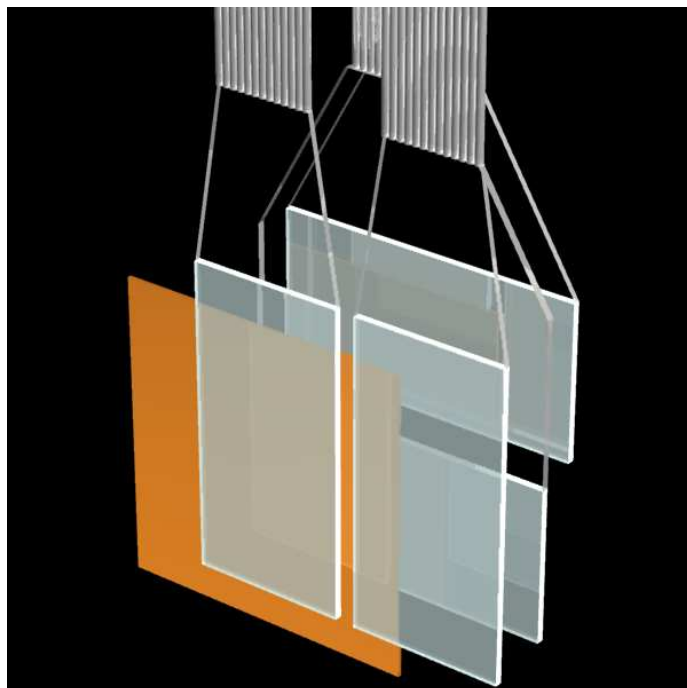


Figure 2.10: A schematic view of a front counter (FC). Two pairs of plastic scintillators segmented in vertical and horizontal directions are indicated by light blue rectangles. A copper plate of 0.5 mm thickness is inserted between the pairs. The scintillator light outputs are fed to PMTs via an acrylic light guide and optical fibers.